Journal of Thermal Stresses, 31: 1006–1021, 2008
Copyright © Taylor & Francis Group, LLC
ISSN: 0149-5739 print/1521-074X online
DOI: 10.1080/01495730802250714

Taylor & Francis
Taylor & Francis Group

Downloaded By: [Batra, R. C.] At: 12:55 3 October 2008

PULL-IN INSTABILITIES IN FUNCTIONALLY GRADED MICROTHERMOELECTROMECHANICAL SYSTEMS

D. J. Hasanyan[1], R. C. Batra[1], and S. Harutyunyan[2]
[1]*Department of Engineering Science and Mechanics, Virginia Polytechnic Institute & State University, Blacksburg, Virginia, USA*
[2]*Materials Science and Engineering Department, Virginia Polytechnic Institute & State University, Blacksburg, Virginia, USA*

We study pull-in instabilities in a functionally graded microelectromechanical system (MEMS) due to the heat produced by the electric current. Material properties of two-phase MEMS are assumed to vary continuously in the thickness direction. It is shown that the pull-in voltage strongly depends upon the variation through the thickness of the volume fractions of the two constituents. It is probably the first work to consider Joule's heating, dependence of the electric conductivity upon the temperature, and the gradation of material properties in studying the pull-in instability in micro-thermo-electro-mechanical plates.

Keywords: Coupled thermo-electric problems; Functionally graded materials; Microelectromechanical system

INTRODUCTION

Electrostatically actuated microelectromechanical systems (MEMS) are used as transistors, switches, micro-mirrors, pressure sensors, micro-pumps, and micro-grippers, see e.g., [1–4]. MEMS are usually comprised of a conductive deformable body suspended above a rigid grounded body [5]. An applied direct current potential difference between the two bodies induces the Coulomb force that deflects the deformable body, and consequently changes the system capacitance. When an additional alternating current is applied to excite harmonic motions of the deformable electrode, resonant devices are obtained. These devices are used in signal filtering, and chemical and mass sensing, see e.g., [6–9]. The applied direct current voltage has an upper limit beyond which the electrostatic force is not balanced by the elastic restoring force in the deformable conductor, and the MEMS

Received 5 March 2008; accepted 15 May 2008.
This work was partially supported by Virginia Tech's Institute of Critical Technologies and Applied Sciences and the Office of Naval Research Grant No. N00014-98-06-0567 to Virginia Polytechnic Institute and State University with Dr. Y.D.S. Rajapakse as the program manager. Views expressed in the paper are those of the authors, and not of the funding agency or of the program manager or of their institutions.
Address correspondence to R. C. Batra, Department of Engineering Science and Mechanics, M/C 0219, Virginia Polytechnic Institute & State University, Blacksburg, VA 24061, USA. E-mail: rbatra@vt.edu

eventually collapses. This phenomenon, called pull-in instability, has been observed experimentally [10, 11]. The critical voltage associated with this instability is called the pull-in voltage. In micro-mirrors [2] and micro-resonators [12] the designer avoids this instability to achieve stable motions, while in switching applications [1] the designer exploits this effect to optimize device's performance. Much of the literature on MEMS is summarized in [13], and the pull-in instability in MEM plates and membranes has been studied by several researchers; e.g., see [14–16] and references cited therein.

The MEMS are typically laminated structures, and their desired performance is achieved by varying the ply thickness, its material (silicon based materials), and the stacking sequence [17–19]. Here we propose that they be comprised of functionally graded materials (FGMs) in which material properties vary continuously through the thickness. This is achieved by using two or more materials and varying continuously their volume fractions. Such a design precludes the well-known shortcomings (e.g., delamination and debonding) of laminated structures. Moreover FGMs can be used in severe thermal environments.

Nearly all of the research work on MEMS has assumed that the two plates are perfect conductors with no current flowing through the plates. Consequently, the thermal management problem has not been addressed. We consider Joule's heating, and study the pull-in instability induced by temperature rise in FG MEMS comprised of two parallel flat plates. In order to simplify the problem we regard both plates to be rigid. Because of the dependence of the electric conductivity upon the temperature, the non-linear equations governing the heat and the current flow in a plate are two-way coupled. The pull-in voltage is defined as the minimum voltage that results in an unbounded monotonic rise in the temperature of the plate. A future study will combine the thermal, mechanical and electrical effects.

Downloaded By: [Batra, R. C.] At: 12:55 3 October 2008

FORMULATION OF THE PROBLEM

We consider an isotropic micro-thermo-electro-mechanical plate (MTEMP) of thickness $2h$ and length $2a$ with voltage difference V applied to the edges $x_1 = -a$ and $x_1 = a$ as shown in Figure 1. Our primary interest is to analyze the effect of Joule's heating on the pull-in instability. Accordingly, we neglect mechanical deformations of the plate, assume it to be isotropic, electrically and thermally

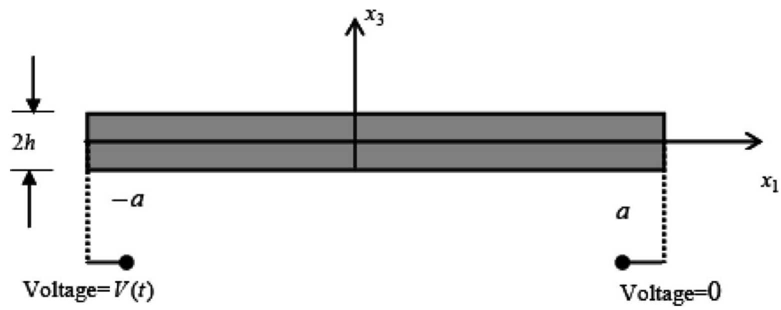

Figure 1 Functionally graded MTEMP.

conducting, and analyze coupled thermal and electrical fields. The simple geometry and the assumption of the plate being rigid allow us to analyze and capture many effects exhibited by a MTEMP. We assume that the plate dimension in the x_2-direction is much larger than $2a$ and $2h$, the thermal and the electrical conductivities of the material vary smoothly in the x_3- and the x_1-directions, and the electrical conductivity of the material may depend upon the temperature.

The coupled thermo-electric fields in the plate are found by simultaneously solving the Maxwell Eq. (1a) and the heat conduction Eq. (1b).

$$\nabla \cdot (\sigma \nabla \psi) = 0 \tag{1a}$$

$$\nabla \cdot (\lambda \nabla T) + \sigma |\nabla \psi|^2 - c_e \dot{T} = 0 \tag{1b}$$

The electrical field $\mathbf{E}$ is related to the electrostatic potential ψ by $\mathbf{E} = -\nabla\psi$ where $\nabla = (\partial/\partial x_1, \partial/\partial x_3)$ is the in-plane gradient operator. Furthermore, σ is the electric conductivity, $\mathbf{J} = \sigma\mathbf{E}$ the electric current, T the temperature, $\lambda = \lambda(x_1, x_3)$ the thermal conductivity, $c_e = c_e(x_1, x_3)$ the specific heat capacity of the material, and a superimposed dot indicates differentiation with respect to time t. In Eq. (1a) we have neglected inertia associated with the electrical field. This is justified since the time scale for the electric problem is much smaller than that for the thermal problem. The potential ψ and the temperature T are taken to satisfy the following initial and boundary conditions:

$$\psi(a, x_3, t) = 0, \quad \psi(-a, x_3, t) = V(t), \quad \psi(x_1, \pm h, t) = 0 \tag{2a}$$

$$\begin{aligned} &T(x_1, x_3, t)|_{t=0} = 0 \\ &\lambda(x_1, \pm h)\partial T/\partial x_3|_{x_1=\pm h} = \mp\gamma(x_1, \pm h)(T - T_A)|_{x_1=\pm h} \\ &\lambda(\pm a, x_3)\partial T/\partial x_1|_{x_1=\pm a} = 0 \end{aligned} \tag{2b}$$

Here T_A is the temperature of the surrounding environment, and $\gamma(x_1, \pm h)$ is the heat transfer coefficient of the surfaces $x_3 = \pm h$. We note that the electrical and the thermal boundary conditions at the corners are ambiguous, since these points belong to two surfaces with different boundary conditions prescribed on them. Boundary conditions (2a) and (2b) imply that the top and the bottom surfaces of the plate are grounded and exchange heat with the surroundings through convective type boundary conditions. The left and the right edges of the plate are thermally insulated, the right edge is grounded, and the left edge surface is held at a time-dependent voltage $V(t)$.

We assume that the electrical conductivity, the thermal conductivity, and the specific heat can be expressed as

$$\begin{aligned} &\sigma = \sigma(x_1, x_3, T) = \sigma_0(x_3) f(x_1, T), \\ &\lambda(x_1, x_3) = \lambda(x_3), \\ &c_e(x_1, x_3) = c_e(x_3), \end{aligned} \tag{3}$$

where $\sigma_0(x_3)$ is the electrical conductivity at the ambient temperature, and $f = f(T) = \exp(T)$ is a continuous function of temperature and does not depend

Downloaded By: [Batra, R. C.] At: 12:55 3 October 2008

on the x_1-coordinate. Exponential dependence of the thermal conductivity upon the temperature is valid for materials used to fabricate Joule heaters, e.g., silicon nitride (SiN) is one such material. We note that for undoped silicon, the electrical conductivity decreases with a rise in temperature. When the electrical conductivity varies with the temperature, Eqs. (1a) and (1b) are two-way coupled. However, when the electrical conductivity is independent of temperature, then these two equations are one-way coupled in the sense that the electric field can first be found by solving Eq. (1a) under the prescribed boundary conditions, and then the temperature field can be computed from Eq. (1b).

Downloaded By: [Batra, R. C.] At: 12:55 3 October 2008

Reduced-Order Models of the Problem

Even with the afore-stated simplifying assumptions, we are unable to solve the problem analytically. We employ an asymptotic expansion of the field variables and investigate characteristics of the solution for a range of parameter values. Said differently, we derive a variable-order plate theory for a plate made of a nonlinear thermo-electric material.

Postulating that ψ and T are analytic functions of the thickness coordinate x_3, we expand them as

$$\psi(x_1, x_3, t)/V_0 = \sum_{i=0}^{N} \psi_i(x_1, t)(x_3)^i, \quad T(x_1, x_3, t)/T_A = \sum_{i=0}^{N} T_i(x_1, t)(x_3)^i \tag{4}$$

where $V_0 = V(0)$ equals the initial voltage applied to the left edge of the plate. Note that no *a priori* assumption has been made about the solution of the problem being symmetric with respect to x_1 and x_3. For a FG plate with volume fractions of constituents and hence material properties varying through the plate thickness, the solution, in general, will not be symmetric about the midsurface of the plate even if boundary conditions on the top and the bottom surface are the same. Substitution from Eq. (4) into Eqs. (1) through (3) and using the analogue of the principle of virtual work (see [20–23]), we get a system of nonlinear coupled partial differential equations for ψ_i and T_i $(i = 0, 1, \ldots, N)$. These equations are also too difficult to solve analytically.

Second-Order Reduced Model

We now find a further reduced-order model of the problem by retaining only two terms in series (4), i.e.,

$$\psi(x_1, x_3, t)/V_0 = \psi_0(x_1, t) + x_3\psi_1(x_1, t), \quad T(x_1, x_3, t)/T_A = T_0(x_1, t) + x_3 T_1(x_1, t)$$

and assume that

$$f(T) = f(T_0) + x_3 T_1 f'(T_0)$$

where $f'(T_0) = \frac{df}{dT}\big|_{T=T_0}$. Substituting these expressions in Eqs. (1a, 1b), integrating over the plate thickness the resulting equation and also the equation obtained by multiplying them with x_3, (or equivalently taking the weight function to be $\delta\psi_0 + x_3\delta\psi_1$ for Eq. (1a) and $\delta T_0 + x_3\delta T_1$ for Eq. (1b)) we get the following four partial differential equations for the four unknowns $\psi_i(x_1, t)$ and $T_i(x_1, t)$, $(i = 0, 1)$.

The electrostatic Eq. (1a) yields

$$\frac{\partial}{\partial x_1}\left[f(T_0)\frac{\partial\psi_0}{\partial x_1}\right] + \frac{1}{2h}\left[f(T)\frac{\partial\psi}{\partial x_1}\bigg|_{x_3=h} - f(T)\frac{\partial\psi}{\partial x_1}\bigg|_{x_3=-h}\right]$$
$$+ f(T_0)\psi_1\frac{1}{2h}\int_{-h}^{h}\frac{\sigma_0'(x_3)}{\sigma_0(x_3)}dx_3 = 0 \tag{5a}$$

$$\frac{\partial}{\partial x_1}\left[f(T_0)\frac{\partial\psi_1}{\partial x_1}\right] + \frac{\partial}{\partial x_1}\left[f'(T_0)T_1\frac{\partial\psi_0}{\partial x_1}\right] + \frac{3}{2h^2}\left[f(T)\frac{\partial\psi}{\partial x_3}\bigg|_{x_3=h} + f(T)\frac{\partial\psi}{\partial x_3}\bigg|_{x_3=-h}\right]$$
$$+ \frac{3}{2h^3}\left\{f(T_0)\int_{-h}^{h}\frac{x_3\sigma_0'(x_3)}{\sigma_0(x_3)}dx_3 + T_1 f'(T_0)\int_{-h}^{h}\frac{x_3^2\sigma_0'(x_3)}{\sigma_0(x_3)}dx_3\right\}\psi_1$$
$$- \frac{3}{h^2}\psi_1 f(T_0) = 0 \tag{5b}$$

where $\sigma_0'(x_3) = d\sigma_0/dx_3$, and σ_0 is assumed not to vanish. Furthermore, in the derivation of these equations, terms containing the product $\psi_1 T_1$ have been neglected since these terms are of higher order in h/a than those retained in Eqs. (5a, 5b). By following the same procedure as that used to derive Eqs. (5a, 5b) from Eq. (1a), we obtain the following from the thermal Eq. (1b):

$$\frac{\partial^2 T_0}{\partial x_1^2} + T_1\frac{1}{2h}\int_{-h}^{h}\frac{\lambda'(x_3)}{\lambda(x_3)}dx_3 + f(T_0)\left[\left(\frac{\partial\psi_0}{\partial x_1}\right)^2 + \psi_1^2\right]\frac{1}{2h}\int_{-h}^{h}\frac{\sigma_0(x_3)}{\lambda(x_3)}dx_3$$
$$+ \left\{T_1 f'(T_0)\left[\left(\frac{\partial\psi_0}{\partial x_1}\right)^2 + \psi_1^2\right] + 2f(T_0)\frac{\partial\psi_0}{\partial x_1}\frac{\partial\psi_1}{\partial x_1}\right\}\frac{1}{2h}\int_{-h}^{h}\frac{x_3\sigma_0(x_3)}{\lambda(x_3)}dx_3$$
$$- \frac{\partial T_0}{\partial t}\frac{1}{2h}\int_{-h}^{h}\frac{c_e(x_3)}{\lambda(x_3)}dx_3 - \frac{\partial T_1}{\partial t}\frac{1}{2h}\int_{-h}^{h}\frac{c_e(x_3)}{\lambda(x_3)}x_3 dx_3$$
$$+ \frac{1}{2h}\left[\frac{\partial T}{\partial x_3}\bigg|_{x_3=h} - \frac{\partial T}{\partial x_3}\bigg|_{x_3=-h}\right] = 0 \tag{6a}$$

$$\frac{\partial^2 T_1}{\partial x_1^2} + T_1\frac{3}{2h^2}\int_{-h}^{h}\frac{x_3\lambda'(x_3)}{\lambda(x_3)}dx_3 + f(T_0)\left[\left(\frac{\partial\psi_0}{\partial x_1}\right)^2 + \psi_1^2\right]\frac{3}{2h^2}\int_{-h}^{h}\frac{x_3\sigma_0(x_3)}{\lambda(x_3)}dx_3$$
$$- \frac{3}{h^2}T_1 - \frac{\partial T_0}{\partial t}\frac{3}{2h^3}\int_{-h}^{h}x_3\frac{c_e(x_3)}{\lambda(x_3)}dx_3 - \frac{\partial T_1}{\partial t}\frac{3}{2h^3}\int_{-h}^{h}\frac{c_e(x_3)}{\lambda(x_3)}x_3^2 dx_3$$
$$+ \frac{3}{2h^2}\left[\frac{\partial T}{\partial x_3}\bigg|_{x_3=h} + \frac{\partial T}{\partial x_3}\bigg|_{x_3=-h}\right]$$
$$+ f'(T_0)T_1\left[\left(\frac{\partial\psi_0}{\partial x_1}\right)^2 + \psi_1^2\right]\frac{3}{2h^3}\int_{-h}^{h}\frac{x_3^2\sigma_0(x_3)}{\lambda(x_3)}dx_3 = 0 \tag{6b}$$

The coupled system of Eqs. (5a, 5b) and (6a, 6b) is still too difficult to solve analytically.

Downloaded By: [Batra, R. C.] At: 12:55 3 October 2008

Membrane Approximation

To get qualitative results, we further reduce the number of unknown functions by assuming that $\psi_1(x_1, t) \approx 0$ and $T_1(x_1, t) \approx 0$. Terms related to functions $\psi_1(x_1, t)$ and $T_1(x_1, t)$ are of the order (h/a) but those involving $\psi_0(x_1, t)$ and $T_0(x_1, t)$ are of order 1. This approximation models the MTEM as a membrane, and is quite good for $(h/a) \leq 1/100$. Several works (e.g., see [15, 16]) have used a membrane approximation for the deformable electrode in a MEMS. Equations for the determination of $\psi_0(x_1, t)$ and $T_0(x_1, t)$ deduced from Eqs. (5a) and (6a) by neglecting terms involving ψ_1 and T_1 are

$$\frac{\partial}{\partial x_1}\left[f(T_0)\frac{\partial \psi_0}{\partial x_1}\right] + \frac{1}{2h}\left[f(T_0)\frac{\partial \psi_0}{\partial x_1}\bigg|_{x_3=h} - f(T_0)\frac{\partial \psi_0}{\partial x_1}\bigg|_{x_3=-h}\right] = 0 \tag{7a}$$

$$\frac{\partial^2 T_0}{\partial x_1^2} + f(T_0)\left(\frac{\partial \psi_0}{\partial x_1}\right)^2 \frac{1}{2h}\int_{-h}^{h} \frac{\sigma_0(x_3)}{\lambda(x_3)}dx_3 - \frac{\partial T_0}{\partial t}\frac{1}{2h}\int_{-h}^{h}\frac{c_e(x_3)}{\lambda(x_3)}dx_3$$
$$+ \frac{1}{2h}\left[\frac{\partial T_0}{\partial x_3}\bigg|_{x_3=h} - \frac{\partial T_0}{\partial x_3}\bigg|_{x_3=-h}\right] = 0 \tag{7b}$$

Integrating Eq. (7a) with respect to x_1 and using boundary conditions (2a), we get the following from Eq. (7a):

$$\frac{\partial \psi_0}{\partial x_1} = \frac{V_0(t)}{f(T_0)\int_{-a}^{a}(1/f(T_0))dx_1} \tag{8}$$

Inserting Eq. (8) into Eq. (7b), and using boundary conditions (2b) we obtain the following nonlinear and nonlocal equation in terms of non-dimensional variables:

$$\frac{\partial \theta}{\partial \tau} = F(\theta, \tau) + \alpha\frac{\partial^2 \theta}{\partial x^2} \tag{9a}$$

where

$$F(\theta, \tau) = -\theta + P_0 V^2(\tau)\Bigg/\left(V_0 f(\theta)\left[\int_{-1}^{1}(1/f(\theta))dx\right]^2\right), \quad \theta = (T_0 - T_A)/T_A \tag{9b}$$

$$P_0 = \frac{V_0^2\tilde{\sigma}_0\alpha}{T_A}, \quad \alpha = \frac{2h^2}{a^2}\frac{1}{Bi(h) + Bi(-h)}, \quad \tilde{\sigma}_0 = \frac{1}{2h}\int_{-h}^{h}\frac{\sigma_0(x_3)dx_3}{\lambda(x_3)},$$

$$Bi(\pm h) = \frac{h\gamma(\pm h)}{\lambda(\pm h)}$$

$$\tau = a^2 t/(\alpha\tilde{c}_0), \quad \tilde{c}_0 = \frac{1}{2h}\int_{-h}^{h}\frac{c_e(x_3)}{\lambda(x_3)}dx_3, \quad x = x_1/a, \quad V(\tau) = V(\tau)/V_0, \tag{10a-i}$$

$Bi(h)$ and $Bi(-h)$ are the Biot numbers of the top and the bottom surfaces, respectively. We note that equations similar to Eqs. (9) arise in combustion and chemical reaction theory, and in the analysis of microwave heating of structural elements [17].

Downloaded By: [Batra, R. C.] At: 12:55 3 October 2008

Boundary and initial conditions for Eq. (9a) are

$$\left.\frac{\partial\theta}{\partial x}\right|_{x=\pm1} = 0, \quad \theta|_{\tau=0} = 0 \tag{11}$$

Series Solution of Eq. (9a)

We assume that

$$\theta(x,\tau) = \sum_{m=0}^{\infty} \theta_m(\tau)\varphi_m(x) \tag{12}$$

where $\varphi_m(x) = \cos(\lambda_m x)$ with $\lambda_m = \pi m, (m = 0, \pm1, \dots)$ are shape functions satisfying boundary conditions (11). The application of Galerkin's method to Eq. (9a) gives the following nonlinear system of ordinary differential equations:

$$\frac{d\theta_m}{d\tau} + \alpha\lambda_m^2\theta_m = G_m(\theta_0, \theta_1, \theta_2, \dots, \theta_n, \dots, \tau), \quad (m = 0, \pm1, \dots) \tag{13}$$

where

$$G_m(\theta_0, \theta_1, \dots, \theta_n, \dots, \tau) = \int_{-1}^{1} \varphi_m(x) F\left(\sum_{n=0}^{\infty} \theta_n(\tau)\varphi_n(x), \tau\right) dx$$

Pull-in Instability and Pull-in Voltage

Equations (9a) and (9b) imply that when P_0 (or the applied initial voltage V_0) is small, the energy input into the system is sufficiently small and the heat transferred out from the top and the bottom surfaces of the plate is enough to establish thermal equilibrium. As P_0 is increased, the heat generated increases, and it eventually overwhelms the heat transferred out from the top and the bottom surfaces of the plate. Thus, the thermal equilibrium can not be established. In microwave heating or in combustion, this phenomenon is called thermal run away. Whether or not this phenomenon occurs in a MTEMP depends upon the range of P_0 (or V_0) in which the device operates and on the dependence of the electrical conductivity upon the temperature. *The maximum value of the applied voltage V_0 for which the energy input into the plate equals that radiated out of its top and bottom surfaces is called the pull-in voltage.* Said differently, when the applied voltage exceeds the pull-in voltage, a steady state distribution of temperature in the plate can not be achieved. The pull-in instability severely restricts the range of stable operation of a device. Here, a mathematical model of an idealized electrostatically actuated MTEM device has been constructed to find the pull-in voltage which is characterized in terms of the bifurcation diagram. We delineate below the pull-in voltage for several cases.

Case I. $\partial\theta/\partial x = 0$, $V(\tau) = 1$ (i.e., $V(t) = V_0 = \text{const}$). In this case $\theta(x,\tau) = \theta(\tau)$, and the entire plate is at the same temperature. Equations (9a) and (9b) reduce to the ordinary differential equation

$$\frac{d\theta}{d\tau} = -\theta + \frac{1}{4}P_0\exp(\theta) \tag{14}$$

Downloaded By: [Batra, R. C.] At: 12:55 3 October 2008

with initial condition

$$\theta|_{\tau=0} = 0 \tag{15}$$

From a numerical solution of Eqs. (14) and (15) computed with *MATHEMATICA*, we conclude the following: (a) if $P_0 > P_{0*}^I = 4/e(\approx 1.471)$ no steady-state solution of Eq. (14) exists, and starting from the initial temperature $\theta(0) = 0$, the temperature continues to increase with time; (b) For $P_0 < P_{0*}^I = 4/e(\approx 1.471)$ the problem has two steady-state solutions θ_{01} and θ_{02} that satisfy the transcendental equation

$$-4\theta + P_0 \exp(\theta) = 0 \tag{16}$$

Assuming that $\theta_{01} < \theta_{02}$, we can verify that the first solution is stable, and the second is unstable. Figure 2 exhibits the bifurcation diagram for this problem. For an initial value $\theta(0) = \theta_0 < \theta_{01}$ and for $P_0 < P_{0*}^I(=4/e)$, the solution monotonically approaches the stable branch, and for $P_0 > P_{0*}^I(=4/e)$ it increases monotonically with time, and becomes unbounded. In the latter case, the device components often stick together or break leading to its failure. This instability severely restricts the range of stable operation of the device.

The time history of evolution of the temperature plotted in Figure 3 shows that for the parameter $P_0 = 1.47 < P_{0*}^I$ the temperature θ stays bounded, and for $P_0 = 1.5 > P_{0*}^I$, the temperature θ becomes unbounded as time increases. Thus the pull-in instability occurs at $P_0 = P_{0*}^I$.

Case II. $\partial\theta/\partial x \neq 0$ and $V(t) = V_0 =$ const. i.e., $V(\tau) = 1$. In this case there is a constant step voltage V_0 applied instantaneously at the left edge of the plate. The number i of terms retained in the series expansion (12) depends upon the values of P_0 and α. When P_0 is close to P_{0*} we need to retain more terms in (12) to satisfy the convergence condition, $|\theta_{i+1}(x, \tau) - \theta_i(x, \tau)|/|\theta_i(x, \tau)| < 10^{-3}$, when $x \in (-1, 1)$ and $\tau > 0$. If $P_0 < P_{0*}$ the convergence condition is satisfied for $i = 4$.

The numerical solution of Eqs. (12) and (13) reveals that values of parameter α (for real materials $\alpha \in (10^{-7}, 1)$) significantly influence the critical value $P_{0*} = P_{0*}^{II}(\alpha)$

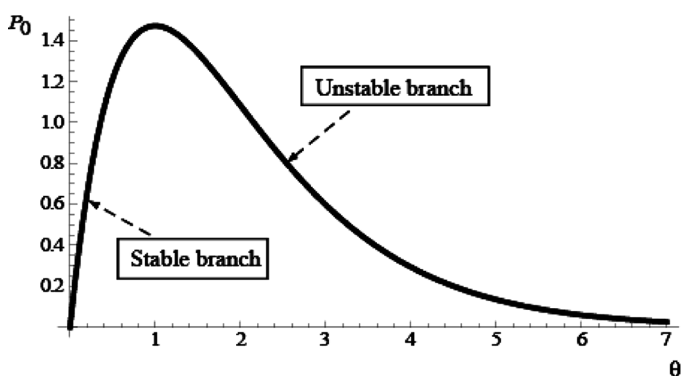

Figure 2 Bifurcation diagram for the membrane model of the MTEMP.

Downloaded By: [Batra, R. C.] At: 12:55 3 October 2008

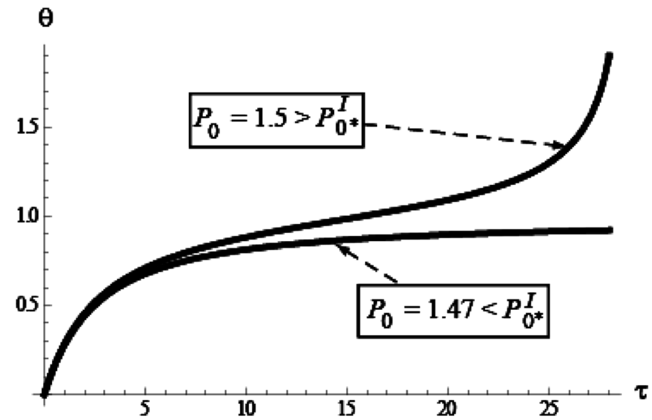

Figure 3 Dependence of non-dimensional temperature θ on non-dimensional time τ.

Downloaded By: [Batra, R. C.] At: 12:55 3 October 2008

of the parameter P_0 for which the temperature becomes unbounded; values of α and corresponding values of P_{0*} are listed in Table 1. For $\alpha \leq 0.01$, P^{II}_{0*} is essentially unchanged and equals 1.5. For $\alpha > 0.01$, P^{II}_{0*} is a monotonically increasing function of α; when α is increased from 0.01 to 0.1, P^{II}_{0*} increases by 22.5%.

For fixed values of the parameter P_0 and three values of the parameter α, we have plotted in Figures 4(a) and (b), the evolution of the temperature $\theta(0, \tau)$ at the centroid of the specimen. These results confirm that for $P_0 < P^{II}_{0*}(\alpha)$ the solution of Eqs. (9a) and (9b) stays bounded, and for $P_0 > P^{II}_{0*}(\alpha)$ the solution becomes unbounded. We note that for the three values of α considered, the value of P_0 is less than its critical value for results plotted in Figure 4(a). The temperature stays bounded till a non-dimensional time of 25 and seems to have reached essentially a steady value. However, for results plotted in Figure 4(b), the value 1.81 of P_0 exceeds its critical value for all three values of α. The temperature of the centroid continues to increase monotonically, and its rapid rate of increase at $\tau = 5$, $\alpha = 10^{-5}$ and 0.05 is evident from the results of Figure 4(b). Recall that P_0 is proportional to the square of the voltage difference applied to the two end faces of the MTEMP.

In Figures 5(a)–(c) we show, for $P_0 = 1.47 < P^{II}_{0*}(0.1)$, the spatial variation of the non-dimensional temperature $\theta(x, \tau)$ for three different values of α and at three non-dimensional times τ. In these cases the non-dimensional temperature $\theta(x, \tau)$ stays bounded. Furthermore, we can conclude that for increasing values of parameter α, the non-dimensional temperature $\theta(x, \tau)$ at a point decreases, and the temperature throughout the specimen eventually becomes uniform, except at the two end faces.

Figures 6(a) and (b) evince the spatial variation of $\theta(x, \tau)$ for $P_0 = 1.81 > P^{II}_{0*}(0.1) = 1.803$, three values of parameters α and two values of the non-dimensional

Table 1 Dependence of $P^{II}_{0*}(\alpha)$ on parameter α

α	10^{-5}	0.01	0.02	0.03	0.04	0.05	0.06	0.07	0.08	0.09	0.1
$P^{II}_{0*}(\alpha)$	1.5	1.51	1.537	1.568	1.599	1.632	1.666	1.7	1.735	1.77	1.803

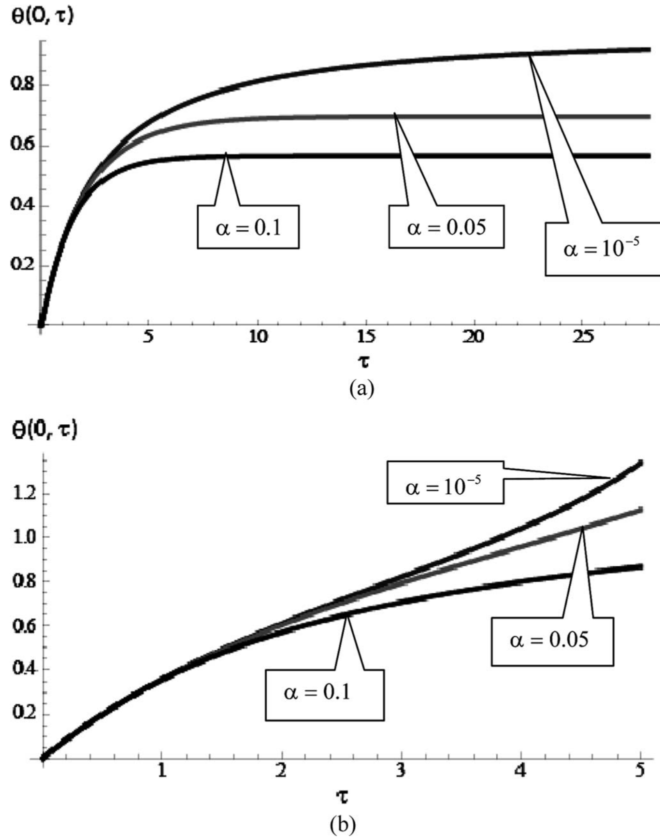

Figure 4 (a) $P_0 = 1.47 < P_{0*}^{II}(10^{-5}) = 1.5$; (b) $P_0 = 1.81 > P_{0*}^{II}(0.1) = 1.803$, and three values of the parameter α, evolution of $\theta(0, \tau)$ with non-dimensional time τ.

Downloaded By: [Batra, R. C.] At: 12:55 3 October 2008

time τ. From these plots we can see that an increase in the value of parameter α decreases the non-dimensional temperature $\theta(x, \tau)$, and the temperature becomes unbounded with an increase in the non-dimensional time τ. The scales along the vertical axis in Figures 5 and 6 are different. Whereas for results depicted in Figure 5 the maximum value of $\theta(x, 30)$ is about 0.92, for results exhibited in Figure 6 $\theta(x, 6)$ and $\theta(x, 6)$ equal 1.33 and 2.05 respectively. Thus when $P_0 > P_{0*}^{II}$, the temperature at every point of the MTEMP becomes very large.

Case III. $\partial\theta/\partial x = 0$, $V(\tau) = \frac{\tau}{\tau_0}H(\tau_0 - \tau) + H(\tau - \tau_0)$. The applied voltage $V(\tau)$ increases linearly from 0 to 1 in non-dimensional time τ_0 and subsequently $V(\tau) = 1$ for $\tau > \tau_0$. The MTEMP is at a uniform temperature. We investigate the effect of the rise time τ_0 on the pull-in instability. The temperature of the body increases uniformly with the passage of time. Values of $P_{0*} = P_{0*}^{III}(\tau_0)$ for five different values of the parameter τ_0 are listed in Table 2. It is clear that the rise time of the applied voltage does not affect much the critical value $P_{0*}^{III}(\tau_0)$ since an increase in the value of the parameter τ_0 from 0 to 10 increases $P_{0*}^{III}(\tau_0)$ by only 0.25%.

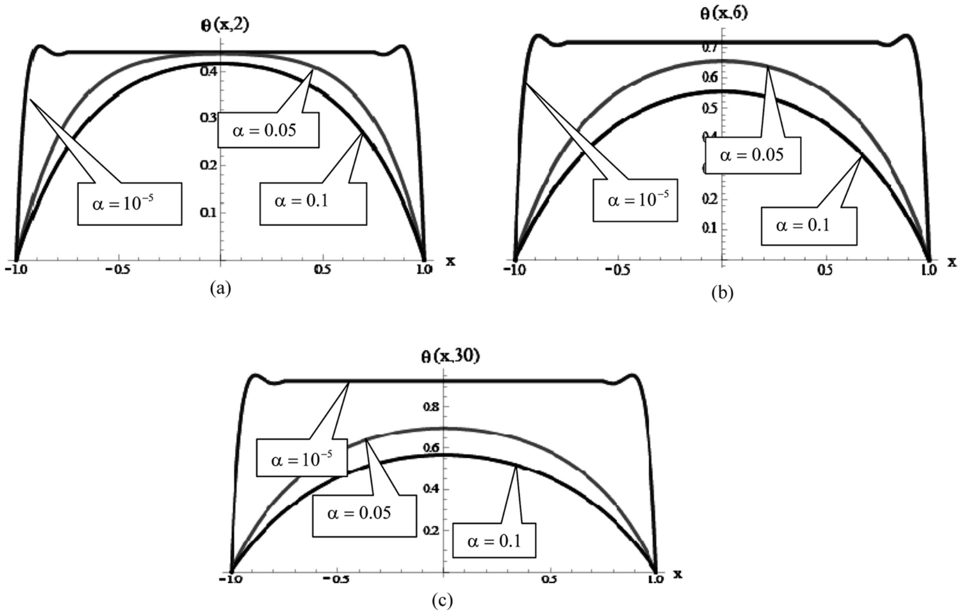

Figure 5 For $P_0 = 1.47 < P_{0*}^{II}(10^{-5})$ and three values of the parameter α, spatial distribution of the temperature at non-dimensional time (a) $\tau = 2$, (b) $\tau = 6$, and (c) $\tau = 30$.

Figures 7(a) and (b) exhibit the evolution of the non-dimensional temperature $\theta(\tau)$ with the non-dimensional time τ. When $P_0 = 1.5 > P_{0*}^{III}(0) = 1.471$, we see that an increase in the rise time enhances the initial temperature rise, eventually the temperature rises unboundedly, and the system becomes unstable. For $P_0 = 1.47 < P_{0*}^{III}(0) = 1.471$, an increase in the value of τ_0 from 0 to 3 has the opposite effect on the initial temperature rise, and eventually the temperatures for the two cases reach the same steady-state value. The initial rise time of the applied voltage has virtually no effect on the critical value of P_{0*}.

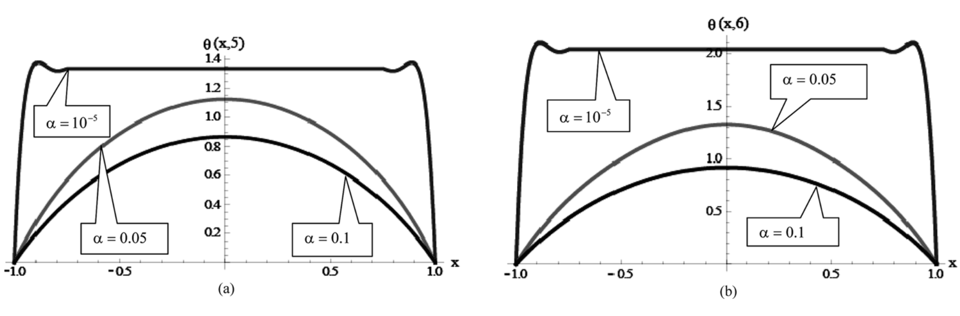

Figure 6 For $P_0 = 1.81 > P_{0*}^{II}(0.1) = 1.803$ and three values of the parameter α, spatial distribution of the temperature at non-dimensional time (a) $\tau = 5$, and (b) $\tau = 6$.

Downloaded By: [Batra, R. C.] At: 12:55 3 October 2008

Table 2 Dependence of the value of $P_{0*}^{III}(\tau_0)$ on the rise time τ_0

τ_0	0	0.01	0.1	1	10
$P_{0*}^{III}(\tau_0)$	1.471	1.47425	1.47426	1.47428	1.47478

Case IV. $\partial\theta/\partial x \neq 0$, $V(\tau) = \cos(\omega\tau)$. For the case of the applied voltage varying harmonically with the non-dimensional frequency ω, Table 3 lists critical values of $P_{0*} = P_{0*}^{IV}(\alpha, \omega)$. For a fixed value of ω, increasing α from 10^{-5} to 10^{-2} has virtually no effect on the value of P_{0*}. However, changing the frequency ω of the applied voltage from 0.01 to 10 increases the value of P_{0*} from 1.54 to 2.999, i.e., by a factor of almost 2.

Results plotted in Figures 8(a) and (b), demonstrate that for a harmonically applied voltage, the temperature rise in the plate is also oscillatory and the amplitude of oscillations stays bounded for $P_0 = 2.5 < P_{0*}^{IV}(0, 1)$ but becomes unbounded when $P_0 = 3.52 > P_{0*}^{IV}(0, 1)$. For the stable solution plotted in Figure 8(a), the frequency of θ is much less than that of the applied voltage $V(\tau)$. For the unstable solution depicted in Figure 8(b), the time period of initial oscillations is considerably more than that of the applied voltage, and the positive amplitude of successive oscillations continues to increase. The temperature becomes negative because the sum of the heat lost to the environment and that conducted away from the point exceeds the heat produced there due to the electric current.

The four cases (I)–(IV) clearly evince that the critical value P_{0*}^{I} of P_0^I for case I is less than that for the other three cases.

Downloaded By: [Batra, R. C.] At: 12:55 3 October 2008

Dependence of the Pull-in Voltage on Gradient of the Plate's Material Properties

We now show that by suitably varying material properties in the thickness direction, we can regulate the pull-in voltage. We assume that the plate is made of two constituents, and use the rule of mixtures to derive effective properties of the

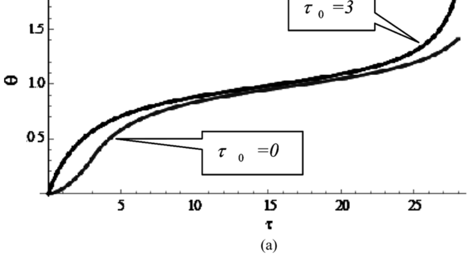

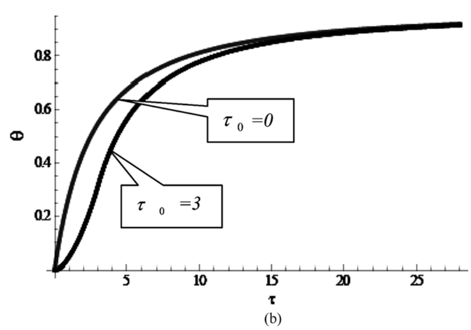

Figure 7 (a) $P_0 = 1.5 > P_{0*}^{III}(0) = 1.471$; (b) $P_0 = 1.47 < P_{0*}^{III}(0) = 1.471$, and two values of the rise time τ_0, evolution of $\theta(0, \tau)$ with non-dimensional time τ.

Table 3 Dependence of $P_{0*}^{IV}(\alpha, \omega)$ on parameters ω and α

	$\alpha = 10^{-5}$	$\alpha = 0.01$
ω	$P_{0*}^{IV}(\alpha, \omega)$	$P_{0*}^{IV}(\alpha, \omega)$
0	1.51	1.511
0.01	1.54	1.547
0.1	2.041	2.046
1	2.829	2.844
10	2.999	3.02

FGM. That is,

$$P(x_3) = P_1[(1 - P_2/P_1)((x_3 + h)/(2h))^m + P_2/P_1] \tag{17}$$

where P_1 and P_2 are values of the material parameter for phases 1 and 2, respectively, and $m(\geq 0)$ is the volume fraction parameter. Thus the bottom surface $x_3 = -h$ of the MTEMP is comprised of material 1, and the top surface $x_3 = h$ of material 2. We presume that for the FG plate, the pull-in voltage for Case I is the least out of the four cases studied above, and assume that the temperature of the plate is a function of time only.

It follows from results given in the previous section that for the critical value P_{0*} of P_0, the solution of Eq. (9a) becomes unbounded for $P_0 > P_{0*}$. By setting $P_0 = P_{0*}$ we get the following expression for the pull-in voltage V_*:

$$\frac{V_{0*}^2 \tilde{\sigma}_0 \alpha}{T_A} = P_{0*} \tag{18}$$

For the two-phase mixture, the non-dimensional pull-in voltage V_* is given by

$$V_*(\sigma, \lambda, m) \equiv \frac{V_{0*}^2}{(1 + Bi)V_{01}^2} = \left[\int_{-1}^{1} \frac{(1-\sigma)(0.5 + 0.5y)^m + \sigma}{(1-\lambda)(0.5 + 0.5y)^m + \lambda} dy\right]^{-1} \tag{19}$$

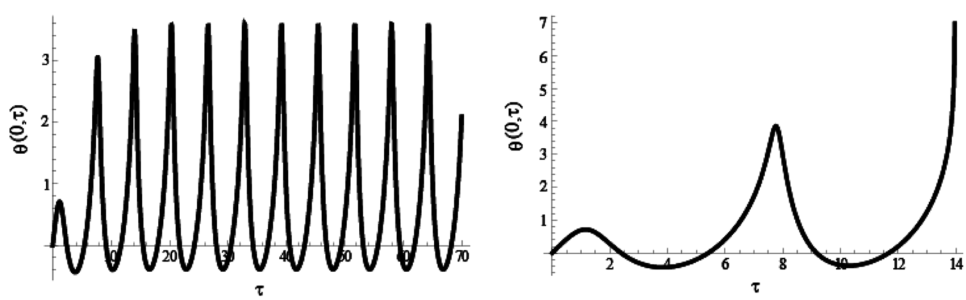

(a) (b)

Figure 8 (a) $P_0 = 2.5 < P_{0*}^{IV}(0, 1)$; (b) $P_0 = 3.52 > P_{0*}^{IV}(0, 1)$ evolution of $\theta(0, \tau)$ with non-dimensional time τ.

Downloaded By: [Batra, R. C.] At: 12:55 3 October 2008

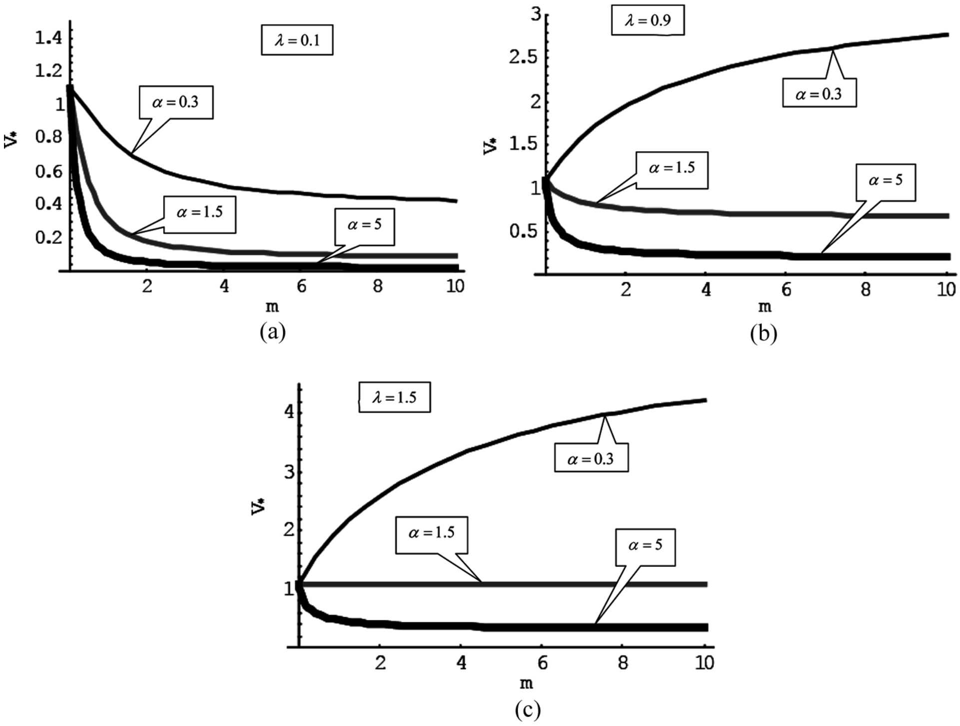

Figure 9 (a) $\lambda = 0.1$; (b) $\lambda = 0.9$; (c) $\lambda = 1.5$ and three values of the electrical conductivity ratio σ, the dependence of the pull-in voltage V_* on the volume fraction exponent m.

where $Bi = Bi_2/Bi_1$, $\sigma = \sigma_{02}/\sigma_{01}$, $\lambda = \lambda_2/\lambda_1$; $V_{01}^2 = P_{0*}T_A a^2 \lambda_1 Bi_1(-h)/(h^2\sigma_{01})$, $y = x_3/h$; $Bi_1 = Bi(-h)$ and $Bi_2 = Bi(h)$ are the Biot numbers for phases 1 and 2 respectively; and V_{01} is the pull-in voltage for a homogeneous plate made of material 1. In Figures 9(a)–(c) the dependence of the non-dimensional pull-in voltage V_* on the volume fraction parameter m for different values of the non-dimensional electrical conductivity σ and the non-dimensional thermal conductivity λ is exhibited. It is clear that the volume fraction parameter m and other material parameters (such as σ and λ) strongly influence the pull-in voltage. For $\lambda = \sigma = 1.5$, the volume fraction exponent m has a negligible effect on the pull-in voltage V_*. The pull-in voltage of a FG plate is quite different from that of the homogeneous plate. By choosing an appropriate value of the volume fraction exponent m and materials of the two phases, one can control the pull-in voltage of the MTEM device.

CONCLUSIONS

We have considered the Joule heating while studying the pull-in instability in an electrically and thermally conducting functionally graded flat plate. Mathematical models of the problem of different complexity have been developed. It has been shown that even the simplest model requires solving simultaneously

Downloaded By: [Batra, R. C.] At: 12:55 3 October 2008

two coupled nonlinear partial differential equations. Depending upon the initial conditions and values of material parameters, the solution of these equations may be stable or unstable. The unstable solution corresponds to the situation when the temperature of the body continues to rise unboundedly in time. The minimum value of the applied voltage that results in the temperature rising monotonically to infinity is called the pull-in voltage. It was found that the pull-in voltage can be regulated by varying volume fractions of the two constituents through the thickness of a functionally graded plate. This is most likely the first work to consider both Joule's heating and gradation of material properties in studying the pull-in instability in micro-thermo-electro-mechanical plates.

REFERENCES

1. C. T. C. Nguyen, L. P. B. Katehi, and G. M. Rebeiz, Micromachined Devices for Wireless Communications, *Proc. IEEE*, vol. 86, pp. 1756–1768, 1998.
2. E. S. Hung and S. D. Senturia, Extending the Travel Range of Analog-tuned Electrostatic Actuators, *J. Microelectromechan. Sys.*, vol. 8, pp. 497–505, 1999.
3. R. K. Gupta and S. D. Senturia, Pull-in Time Dynamics as a Measure of Absolute Pressure, in: *Proc. IEEE Int. Workshop on Microelectromechanical Systems* (*MEMS'97*), Nagoya, Japan, 1997, pp. 290–294.
4. P. B. Chu, P. R. Nelson, M. L. Tachiki, and K. S. Pister, Dynamics of Polysilicon Parallel-Plate Electrostatic Actuators, *Sensor Actuator. A-Phys.*, vol. 52, pp. 216–220, 1996.
5. J. A. Pelesko and D. H. Bernstein, *Modeling MEMS and NEMS*, Chapman & Hall, London, 2002, Chapter 7.
6. J. F. Rhoads, S. W. Shaw, and K. L. Turner, The Nonlinear Response of Resonant Microbeam Systems with Purely-Parametric Electrostatic Actuation, *J. Micromech. Microeng.*, vol. 16, pp. 890–899, 2006.
7. H. A. Tilmans and R. Legtenberg, Electrostatically Driven Vacuum-Encapsulated Polysilicon Resonators: Part II. Theory and Performance, *Sensor Actuator. A Phys.*, vol. 45, pp. 67–84, 1994.
8. J.-H. Kuang and C.-J. Chen, Dynamic Characteristics of Shaped Micro-Actuators Solved Using the Differential Quadrature Method, *J. Micromech. Microeng.*, vol. 14, pp. 647–655, 2004.
9. W. C. Xie, H. P. Lee, and S. P. Lim, Nonlinear Dynamic Analysis of MEMS Switches by Nonlinear Modal Analysis, *Nonlin. Dynam.*, vol. 31, pp. 243–256, 2003.
10. G. I. Taylor, The Coalescence of Closely Spaced Drops When They are at Different Electric Potentials, *Proc. Roy. Soc. London Ser. A*, vol. 306, pp. 423–434, 1968.
11. H. C. Nathanson, W. E. Newell, R. A. Wickstrom, and J. R. Davis, The Resonant Gate Transistor, *IEEE Trans. Electron Devices*, vol. 14, pp. 117–133, 1967.
12. H. A. Tilmans and R. Legtenberg, Electrostatically Driven Vacuum-Encapsulated Polysilicon Resonators: Part I. Design and Fabrication, *Sensor Actuator. A Phys.*, vol. 45, pp. 57–66, 1994.
13. R. C. Batra, M. Porfiri, and D. Spinello, Review of Modeling Electrostatically Actuated Microelectro-mechanical Systems, *Smart Mater. Struct.*, vol. 16, R23–R31, 2007.
14. R. C. Batra, M. Porfiri, and D. Spinello, Reduced-order Models for Microelectromechancial Rectangular and Circular Plates Incorporating the Casimir Force, *Int. J. Solids Struct.*, vol. 45, pp. 3558–3583, 2008.
15. R. C. Batra, M. Porfiri, and D. Spinello, Effects of Casimir Force on Pull-in Instability in Micromembranes, *Europhys. Lett.*, vol. 77, art. no. 20010, 2007.

Downloaded By: [Batra, R. C.] At: 12:55 3 October 2008

16. R. H. Plaut, Linearly Elastic Annular and Circular Membranes Under Radial Transverse, and Torsional Loading. Part I: Large Unwrinkled Axisymmetric Deformations, *Acta Mechanica* (accepted).
17. M. Bao, *Analysis and Design Principles of MEMS Devices*. Elsevier, 2005, 356 pp.
18. J. D. Cressler (Editor), *Silicon Heterostructure Handbook*, Taylor and Francis, 2006, 1227 pp.
19. M. Gad-el-Hak (Editor), *MEMS, Introduction and Fundamentals*. Taylor and Francis, 2006, 457 pp.
20. D. J. Hasanyan, L. Librescu, Z. Qin, and D. R. Ambur, Magneto-Thermo-Elasticity of Geometrically Nonlinear Laminated Composite Plates, Part I: Foundation of the Theory, *J. Sound Vibr.*, vol. 287, pp. 153–175, 2005.
21. L. Librescu, S.-Y. Oh, and O. Song, Thin-Walled Beams Made of Functionally Graded Materials and Operating in a High Temperature Environment: Vibration and Stability. *J. Therm. Stresses*, vol. 28, pp. 649–712, 2005.
22. R. C. Batra and S. Vidoli, Higher-Order Piezoelectric Plate Theory Derived from a Three-Dimensional Variational Principle, *AIAA J.*, vol. 40, pp. 91–104, 2002.
23. L. F. Qian and R. C. Batra, Three-Dimensional Transient Heat Conduction in a Functionally Graded Thick Plate with a Higher-Order Plate Theory and a Meshless Local Petrov-Galerkin Method, *Comput. Mech.*, vol. 35, pp. 214–226, 2005.

Downloaded By: [Batra, R. C.] At: 12:55 3 October 2008